Cyanobacteria and their secondary metabolites in three freshwater reservoirs in the United Kingdom

Daria Filativa[1], Martin R. Jones[2], John A. Haley[3], Oscar Núñez[4,5], Marinella Farré[1], Elisabeth M.-L. Janssen[2*]

[1] Department of Environmental Chemistry, IDAEA-CSIC, 08034 Barcelona, Spain

[2] Department of Environmental Chemistry, Swiss Federal Institute of Aquatic Science and Technology (Eawag), 8600 Dübendorf, Switzerland

[3] Water Quality Strategy, Yorkshire Water, Leeds, United Kingdom

[4] Department of Chemical Engineering and Analytical Chemistry, University of Barcelona, 08028 Barcelona, Spain

[5] Serra Húnter Professor, Generalitat de Catalunya, 08007 Barcelona, Spain

Electronic Supplementary Information

The electronic supplementary information contains 17 pages numbered S1-S17, 3 texts, 4 tables and 11 figures.

List of Text

List of Tables

List of Figures

detected in the lake sample (bottom, blue) as head to tail plots. The *m/z* value and the retention time (RT in min) are noted in the title line.

Figure S8. Comparison of relative intensity over *m/z* range for mass spectrometry fragmentation spectra between anatoxin-a, bioreagent (bottom, blue) and anatoxin-a detected in the lake sample (top, grey) as head to tail plots. The *m/z* value and the retention time (RT in min) are noted in the title line.

Figure S9. Fragmentation spectrum of Cyanopeptolin CP992 at HCD 15, 30, 45% stepped normalised collision energy. Precursor m/z, retention time (RT) and the building block string are noted at the top. The flat structure is shown with annotated building blocks and sites of fragmentation. The table specifies the m/z value and building block fragment that supports the identification of this compound.

Figure S10. Fragmentation spectrum of Anabaenopeptilide 202A at HCD 15, 30, 45% stepped normalised collision energy. Precursor m/z, retention time (RT) and the building block string are noted at the top. The flat structure is shown with annotated building blocks and sites of fragmentation. The table specifies the m/z value and building block fragment that supports the identification of this compound.

Figure S11. Fragmentation spectrum of MC-FL at HCD 15, 30, 45% stepped normalised collision energy. Precursor m/z, retention time (RT) and the building block string are noted at the top. The flat structure is shown with annotated building blocks and sites of fragmentation. The table specifies the m/z value and building block fragment that supports the identification of this compound.

Text S1. Enumeration of cells using the utermohl inverted microscope technique

For biological analyses, 1 L water samples were kept at 4-8°C in the dark after sampling. Taxonomic analysis by microscopy was performed on the day following sampling. Samples were fixed with Lugol's Iodine (10-20 ml per liter sample). Then the samples were pressurized and transferred to a sedimentation tube. After setting, cells in the sample are directly identified and counted applying an inverted microscope.

Text S2. Enumeration of chlorophyll-a

For chlorophyll-a analysis, samples were filtered and extracted with solvent followed by spectrophotometric measurement according to a published method: Book section A8: The determination of chlorophyll 'a' in plant material (phytoplankton), in suspension in water (solvent extraction method), in the book: Aquatic Environments 1980 – Methods for the Examination of Waters and Associated Materials. SBN 0117516740. Briefly, after filtration step using paper filters, pigments were extracted with 14 mL methanol in a glass test tube. The solution was heated until boiling for 10 seconds. After cooling down to room temperature in the darkness, the filter paper was removed and the extract was centrifuged. The chlorophyll-a concentration was determined by spectrophotometric evaluation of the supernatant. Absorbance measurements were carried out at two wavelengths: 665 nm (the maximum absorption of chlorophyll-a), and 750 nm (compensation for 'background turbidity'). The chlorophyll-a content (µg/L) of samples was then quantified as

$$\frac{\mathbf{13.9} \cdot \boldsymbol{A} \cdot \boldsymbol{v}}{\boldsymbol{d} \cdot \boldsymbol{V}}$$

where *A* is a subtraction of absorbance value obtained at 750 nm from the one obtained at 665 nm; v is the volume of the solvent in mL; d is the cell pathlength in cm; V is the volume if the initial filtered sample in liters (see A8.24b in the noted reference). The factor 13.9 is used for approximation to the reciprocal of the specific absorption coefficient at 665 nm for chlorophyll-a in methanol.

Text S3. Measurement of total ammonium, nitrate and phosphate

Total ammonium was measured according to HMSO Methods for the Examination of Waters and Associated Materials, "Ammonia in Waters 1981"(ISBN: 011 7516139). Its concentration was determined spectrophotometrically. Ammonia in the raw drinking water reacted with hypochlorite ions, which were generated from the sodium dichlorocyanurate reagent to form monochloramine. This reacted with salicylate at pH around 10.5 with presence of sodium nitroprusside formed a blue iodophenol-type compound. This was measured at 660 nm. Range of application was between 0.06 and 2 mg/L, with limit of detection (LOD) at 0.0503 mg/L.

Nitrate was measured according to HMSO Methods for the Examination of Waters and Associated Materials, "Oxidised Nitrogen in Waters, 1981" (ISBN: 011 7515930). Its concentration was determined spectrophotometrically. Nitrate ions were reduced to nitrite by hydrazine under alkaline conditions, cupric ions were used as a catalyst. Under acidic conditions, the total nitrite content of the sample was then reacted with sulphanilamide and N-1-Naphthylenediamine dihydrochloride and formed a characteristic pink dye which was read at 540 nm. Range of application was between 0.2 and 20 mg/L, with LOD at 0.1019 mg/L.

Total phosphate was measured according to HMSO Methods for the Examination of Waters and Associated Materials, "Phosphorus in Waters, Effluents and Sewage 1980" (ISBN: 011 7515825). Its concentration was determined spectrophotometrically. Phosphate ions reacted with a solution that contained molybdic acid, trivalent antimony ions and hydrogen ions for formation of a 12-Molybdophosphoric acid. This was reduced by ascorbic acid and gave a phosphomolybdenum blue complex which was is measured at 660 nm. Range of application was between 0.02 and 2 mg/L, with LOD at 0.0091 mg/L.

Table S1. Standard analytical information including: limit of detection (LOD) and limit of quantification (LOQ) in µg/L for the reference standards and bioreagents in nanopure water and lake water from three reservoirs.

Cyanobacterial metabolite	molecular formula	dominant precursor	nanopure		Ingbirchworth		Tophill Low		Embsay	
			LOD (µg/L)	LOQ (µg/L)	LOD (µg/L)	LOQ (µg/L)	LOD (µg/L)	LOQ (µg/L)	LOD (µg/L)	LOQ (µg/L)
MC-LR	$C_{49}H_{74}N_{10}O_{12}$	$[M+H]^+$	0.23	0.71	1.32	3.99	2.92	8.84	0.74	2.26
MC-RR	$C_{49}H_{75}N_{13}O_{12}$	$[M+2H]^{2+}$	0.31	0.94	1.40	4.24	1.45	4.38	0.58	1.76
MC-YR	$C_{52}H_{72}N_{10}O_{13}$	$[M+2H]^{2+}$	0.23	0.71	1.31	3.98	0.95	2.88	1.64	4.97
MC-LA	$C_{46}H_{67}N_7O_{12}$	$[M+H]^+$	0.30	0.89	1.26	3.82	2.02	6.13	1.11	3.38
MC-LF	$C_{52}H_{71}N_7O_{12}$	$[M+H]^+$	0.27	0.83	1.66	5.04	1.44	4.35	1.74	5.28
MC-LY	$C_{52}H_{71}N_7O_{13}$	$[M+H]^+$	0.24	0.72	1.40	4.23	1.68	5.08	1.97	5.97
MC-LW	$C_{54}H_{72}N_8O_{12}$	$[M+H]^+$	0.27	0.83	1.76	5.34	1.37	4.16	1.43	4.33
MC-HilR	$C_{50}H_{76}N_{10}O_{12}$	$[M+H]^+$	0.24	0.71	0.88	2.66	1.82	5.50	0.93	2.83
[D-Asp^3]MC-LR	$C_{48}H_{72}N_{10}O_{12}$	$[M+H]^+$	0.27	0.81	0.70	2.11	1.09	3.31	0.62	1.89
MC-RR 1024 Group[a]	$C_{48}H_{73}N_{13}O_{12}$	$[M+2H]^{2+}$	0.05	0.15	1.25	3.80	0.67	2.02	n.a.	n.a.
Nodularin	$C_{41}H_{60}N_8O_{10}$	$[M+H]^+$	0.25	0.76	1.06	3.23	2.09	6.34	0.47	1.43
Anabaeneopeptin A	$C_{44}H_{57}N_7O_{10}$	$[M+H]^+$	0.25	0.75	11.96	36.26	1.63	4.94	1.06	3.21
Anabaenopeptin B	$C_{41}H_{60}N_{10}O_9$	$[M+H]^+$	0.29	0.88	4.43	13.43	1.21	3.67	0.56	1.70
Oscillamide Y	$C_{45}H_{59}N_7O_{10}$	$[M+H]^+$	0.27	0.81	3.31	10.02	1.76	5.34	1.80	5.47
Cyanopeptolin A	$C_{46}H_{72}N_{10}O_{12}$	$[M+H]^+$	1.01	3.06	2.18	6.62	1.66	5.04	2.35	7.11
Aerucyclamide A	$C_{24}H_{34}N_6O_4S_2$	$[M+H]^+$	0.24	0.74	2.17	6.58	0.92	2.78	3.19	9.66
Aeruginosin 98B	$C_{29}H_{46}N_6O_9S$	$[M+H]^+$	0.35	1.05	n.a.	n.a.	n.a.	n.a.	n.a.	n.a.
Anatoxin-a	$C_{10}H_{15}NO$	$[M+H]^+$	0.08	0.23	n.a.	n.a.	n.a.	n.a.	n.a.	n.a.
Cylindrospermopsin	$C_{15}H_{21}N_5O_7S$	$[M+H]^+$	0.02	0.05	n.a.	n.a.	n.a.	n.a.	n.a.	n.a.

n.a. = not analysed

[a] Microcystin-RR isomeric group 1024 includes: [Dha^7]MC-RR, [Gly^1,D-Asp^3,Dhb^7]MC-Rhar, [DMAdda^5]MC-RR, [D-Asp^3]MC-RR, [D-Asp^3,(E)-Dhb^7]MC-RR

Table S2. Cyanopeptides detected in lake samples and the respective level of confidence in identification, as well as the reference standard or bioreagent used for quantification by class equivalent.

cyanopeptide	molecular formula	dominant precursor	*m/z* of precursor	quantification equivalent	identification level
MC-LR	$C_{49}H_{74}N_{10}O_{12}$	$[M+H]^+$	995.56	standard available	1
[D-Asp^3]MC-LR	$C_{48}H_{72}N_{10}O_{12}$	$[M+H]^+$	981.15	standard available	1
MC-RR	$C_{49}H_{75}N_{13}O_{12}$	$[M+2H]^{2+}$	519.79	standard available	1
MC-RR 1024 Group[a]	$C_{48}H_{73}N_{13}O_{12}$	$[M+2H]^{2+}$	512.78	[D-Asp^3,(E)-Dhb^7]MC-RR	3
MC-HiLR	$C_{50}H_{76}N_{10}O_{12}$	$[M+H]^+$	1009.57	standard available	1
MC-VF	$C_{51}H_{69}N_7O_{12}$	$[M+H]^+$	972.51	MC-LF	3
MC-FL	$C_{52}H_{71}N_7O_{12}$	$[M+H]^+$	986.52	MC-LF	3
[D-Asp^3,(E)-Dhb^7]MC-HtyHty	$C_{56}H_{71}N_7O_{14}$	$[M+H]^+$	1066.51	MC-YR	3
Anabaenopeptin A	$C_{44}H_{57}N_7O_{10}$	$[M+H]^+$	844.42	bioreagent available	1
Anabaenopeptin B	$C_{41}H_{60}N_{10}O_9$	$[M+H]^+$	837.46	bioreagent available	1
Oscillamide Y	$C_{45}H_{59}N_7O_{10}$	$[M+H]^+$	858.44	bioreagent available	1
Anabaenopeptilide 202A	$C_{51}H_{71}N_9O_{15}$	$[M+H]^+$	1050.51	Cyanopeptolin A	3
Anabaenopeptin D	$C_{44}H_{57}N_7O_9$	$[M+H]^+$	828.43	Anabaenopeptin A	3
Anabaenopeptin NZ841	$C_{45}H_{59}N_7O_9$	$[M+H]^+$	842.44	Anabaenopeptin A	3
Anatoxin-a	$C_{10}H_{15}NO$	$[M+H]^+$	166.12	standard available	1
Aeruginosin NOL1	$C_{26}H_{40}N_6O_6$	$[M+H]^+$	533.31	Aeruginosin 98B	3
Aeruginosin 850	$C_{41}H_{66}N_6O_{13}$	$[M+H]^+$	851.48	Aeruginosin 98B	3
Aeruginosin 822	$C_{39}H_{62}N_6O_{13}$	$[M+H]^+$	823.44	Aeruginosin 98B	3
Aeruginosin 98A	$C_{29}H_{45}ClN_6O_9S$	$[M+H]^+$	689.27	Aeruginosin 98B	3
Cyanopeptolin CP992	$C_{49}H_{69}N_9O_{13}$	$[M+H]^+$	992.51	Cyanopeptolin A	3
Microginin 767	$C_{41}H_{61}N_5O_9$	$[M+H]^+$	768.45	MC-LR	3
Microginin KR604	$C_{32}H_{52}N_4O_7$	$[M+H]^+$	605.39	MC-LR	3
Aeruginosamide	$C_{30}H_{48}N_4O_4S$	$[M+H]^+$	561.35	MC-LR	3
Bacteriohopanetetrol	$C_{41}H_{73}NO_8$	$[M+H]^+$	708.54	MC-LR	3
Veraguamide G	$C_{37}H_{62}N_4O_8$	$[M+NH_4]^+$	708.49	MC-LR	3
Micropeptin LH1062	$C_{53}H_{78}N_{10}O_{13}$	$[M+H]^+$	1063.58	MC-LR	3

Nostosin B	$C_{22}H_{37}N_5O_5$	$[M+H]^+$	452.29	MC-LR	3
Almiramide G	$C_{36}H_{64}N_6O_6$	$[M+H]^+$	677.50	MC-LR	3

[a] Microcystin-RR isomeric group 1024 includes: [Dha^7]MC-RR, [Gly^1,D-Asp^3,Dhb^7]MC-Rhar, [DMAdda^5]MC-RR, [D-Asp^3]MC-RR, [D-Asp^3,(E)-Dhb^7]MC-RR

Table S3. Chlorophyll-a, total ammonium, nitrate, total phosphate, and temperature measured in Ingbirchworth reservoir samples in 2019.

Date	Chlorophyll-a, µg/l	Ammonium total, mg/l	Nitrate, mg/l	Phosphate total, mg/l	Temperature, °C
02.01.2019	12			0.03	3.7
10.01.2019	7			0.03	2.6
18.01.2019	13	0.026	4.40	0.03	2.5
21.01.2019	15			0.03	1.7
29.01.2019	19			0.03	0.9
06.02.2019	28			0.03	0.7
15.02.2019	33	0.008	4.29	0.03	1.8
22.02.2019	23			0.03	3.3
25.02.2019	15			0.02	3.4
05.03.2019	13			0.02	3.8
13.03.2019	5			0.03	3.0
21.03.2019	19	0.008	4.59	0.04	4.6
29.03.2019	17			0.03	4.8
01.04.2019	11			0.02	5.2
09.04.2019	9			0.02	7.6
17.04.2019	6	0.024	4.18	0.02	8
25.04.2019	5			0.03	8.2
03.05.2019	6			0.04	9.8
06.05.2019	6			0.02	10.3
14.05.2019	7	0.013	2.91	0.02	9.6
22.05.2019	4			0.02	9.7
30.05.2019	4			0.02	14.1
07.06.2019	4			0.01	14.3
10.06.2019	4			0.03	13.6
18.06.2019	4	0.004	2.44	0.03	12.5
26.06.2019	6			0.04	12.3
04.07.2019	5			0.02	14.7
12.07.2019	6			0.03	14.3
15.07.2019	7	0.047	1.97	0.03	14.8
23.07.2019	4			0.04	16.9
31.07.2019	12			0.08	16.4
08.08.2019	19			0.07	16.7
16.08.2019	20			0.04	16.3
19.08.2019	24	0.026	1.69	0.04	16.3
27.08.2019	14			0.04	15.9
04.09.2019	37			0.03	15.5
12.09.2019	35			0.03	14.5
20.09.2019	21	0.020	0.99	0.03	14.2
23.09.2019	37			0.03	14.3
01.10.2019	17			0.13	13.3
09.10.2019	5			0.06	12.4
17.10.2019	5	0.040	2.37	0.07	11.1
25.10.2019	6			0.05	10.1
28.10.2019	8			0.12	9.5
05.11.2019	4			0.07	8.3
13.11.2019	4			0.07	7
21.11.2019	4	0.040	3.05	0.06	5.8
29.11.2019	4			0.06	6.1
02.12.2019	4			0.06	
10.12.2019	4			0.06	

Table S3. Chlorophyll-a, total ammonium, nitrate, total phosphate, and temperature measured in Tophill Low reservoir samples in 2019.

Date	Chlorophyll-a, µg/l	Ammonium total, mg/l	Nitrate, mg/l	Phosphate total, mg/l	Temperature, °C
08.01.2019		0.047	11.50	0.13	
16.01.2019	11			0.13	
24.01.2019	74	0.004	10.37	0.12	
01.02.2019	76			0.08	
04.02.2019	59	0.005	10.30	0.07	
12.02.2019	35			0.07	
20.02.2019	21	0.043	9.62	0.08	
28.02.2019	13			0.07	
08.03.2019	12	0.055	9.37	0.09	
11.03.2019	17			0.07	
19.03.2019	29	0.014	8.65	0.05	
27.03.2019	46			0.07	
04.04.2019	32	0.066	9.13	0.05	
01.05.2019	4	0.176	7.36	0.10	
09.05.2019	4			0.06	
17.05.2019	16	0.093	7.95	0.07	
20.05.2019	12			0.06	
28.05.2019	9	0.055	7.64	0.03	
05.06.2019				0.03	
13.06.2019	10	0.123	6.91	0.03	
21.06.2019	7			0.04	
24.06.2019	9	0.148	6.33	0.04	
02.07.2019	4			0.10	
10.07.2019	4	0.187	5.47		19.6
18.07.2019	4			0.05	20.6
26.07.2019	9	0.089	4.86	0.05	20.7
29.07.2019	7			0.06	21.6
06.08.2019	12	0.156	4.97	0.05	21.3
14.08.2019	4			0.10	18.9
30.08.2019	10			0.06	18.8
02.09.2019	22	0.038	5.06	0.05	18.8
10.09.2019	8			0.06	16.5
18.09.2019	5	0.023	5.06	0.03	15.9
26.09.2019	4			0.04	16
04.10.2019	4	0.065	4.92	0.04	14.4
07.10.2019	4			0.05	13.8
15.10.2019	4	0.020	5.31	0.04	12.3
23.10.2019	6			0.05	11.3
31.10.2019	4	0.040	6.51	0.05	9.4
08.11.2019	4			0.04	8.8
11.11.2019	4	0.031	7.75	0.06	8.1
19.11.2019	4			0.05	6.8
05.12.2019	4			0.05	
13.12.2019	4	0.037	9.53	0.05	
16.12.2019	5			0.06	
24.12.2019	4	0.031	9.47	0.07	
25.12.2019		0.003	9.76		
26.12.2019		0.037	9.67		
28.12.2019		0.047	9.92		
29.12.2019		0.037	9.71		

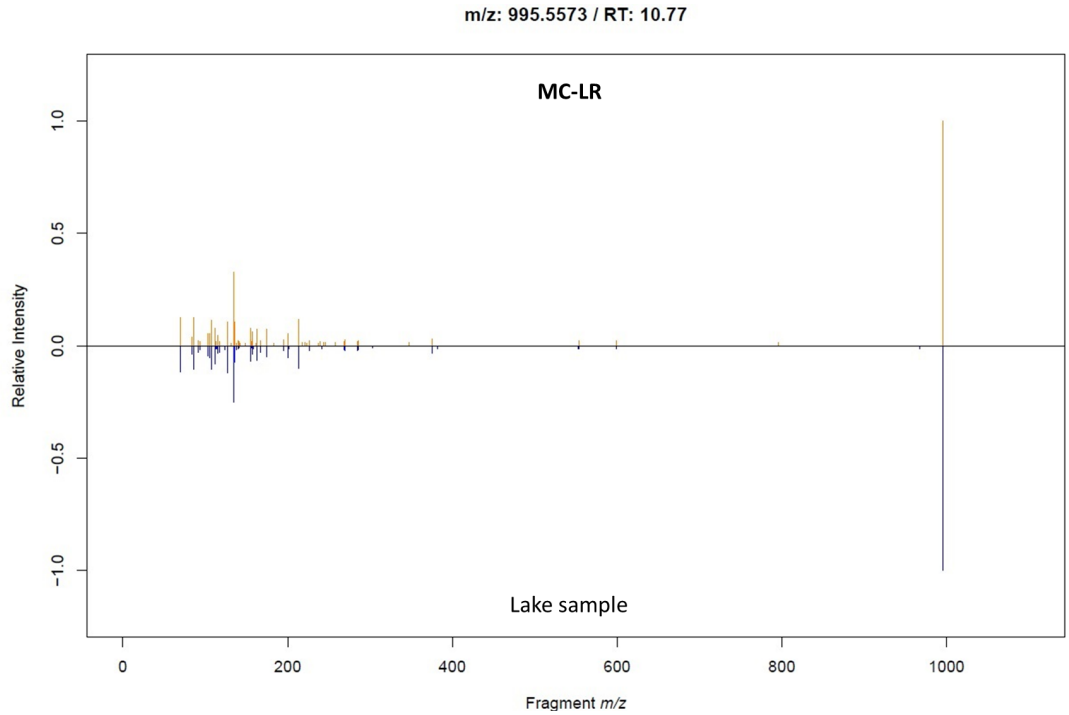

Figure S1. Comparison of relative intensity over *m/z* range for mass spectrometry fragmentation spectra between MC-LR reference standard (top, orange) and MC-LR detected in Ingbirchworth reservoir in the September sample (bottom, blue) as head to tail plot. The *m/z* value and the retention time (RT in min) are noted in the title line, HCD 15, 30, 45% stepped normalised collision energy.

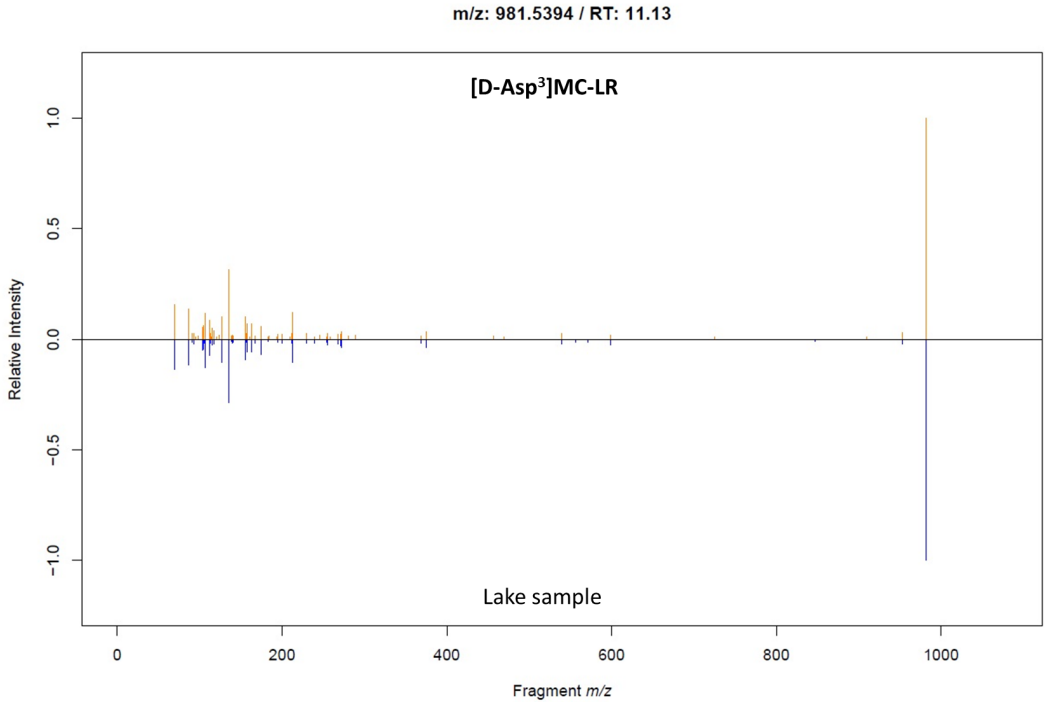

Figure S2. Comparison of relative intensity over *m/z* range for mass spectrometry fragmentation spectra between [D-Asp^3]MC-LR reference standard (top, orange) and [D-Asp^3]MC-LR detected in Ingbirchworth reservoir in the September sample (bottom, blue) as head to tail plots. The *m/z* value and the retention time (RT in min) are noted in the title line, HCD 15, 30, 45% stepped normalised collision energy.

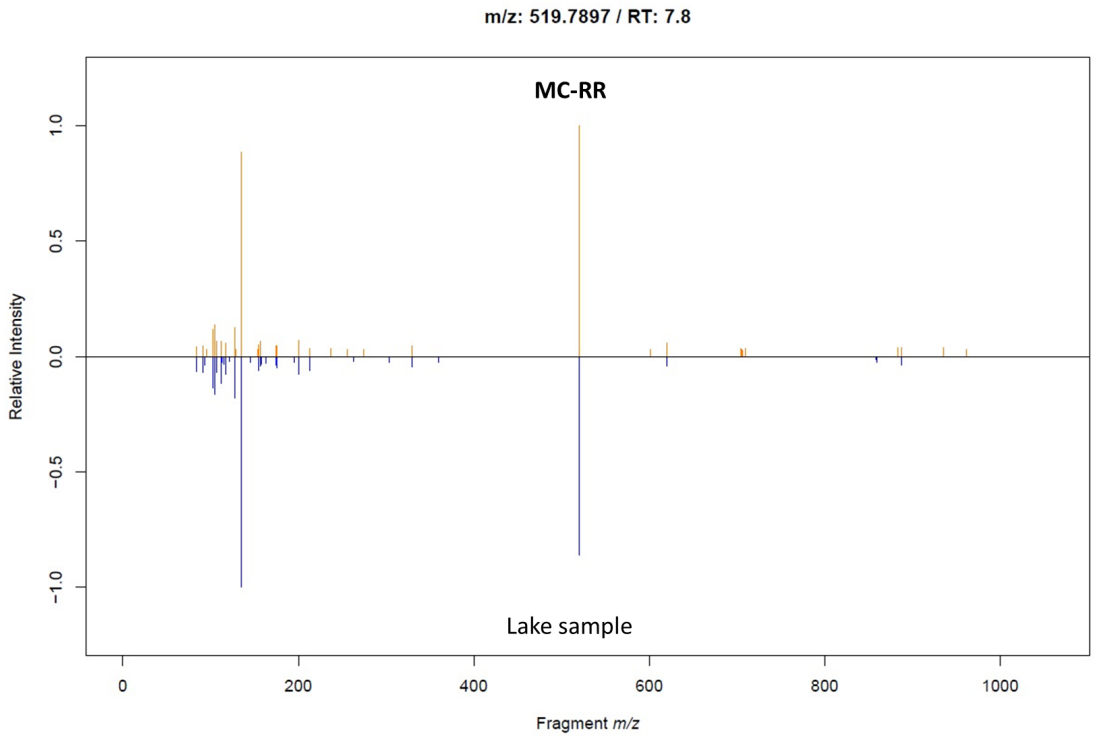

Figure S3. Comparison of relative intensity over *m/z* range for mass spectrometry fragmentation spectra between MC-RR reference standard (top, orange) and MC-RR detected in Ingbirchworth reservoir in the September sample (bottom, blue) as head to tail plots. The *m/z* value and the retention time (RT in min) are noted in the title line, HCD 15, 30, 45% stepped normalised collision energy.

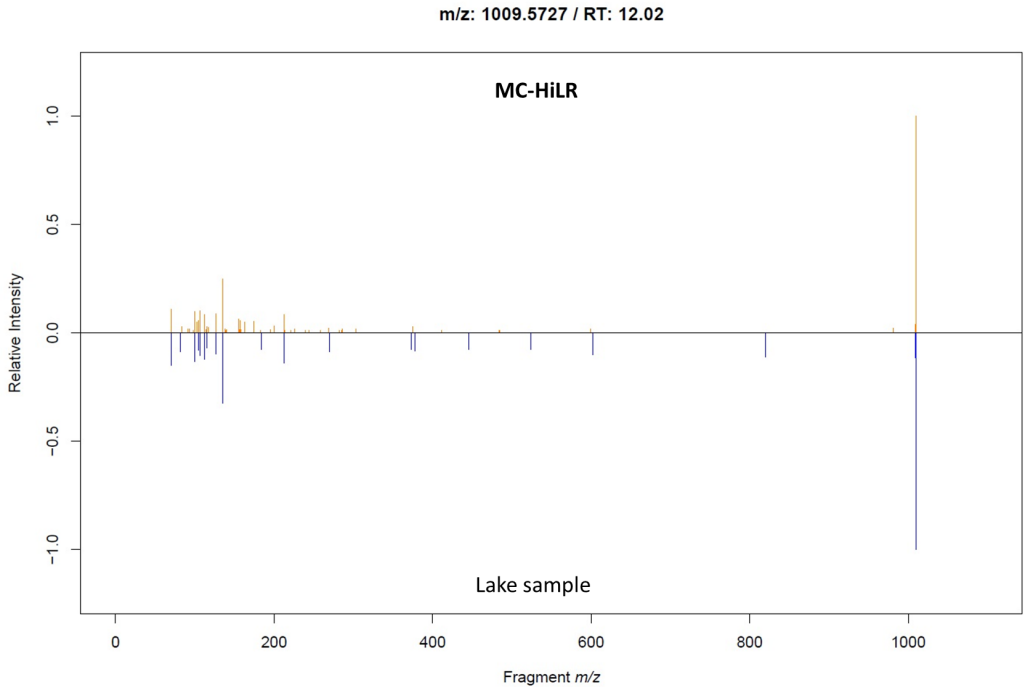

Figure S4. Comparison of relative intensity over *m/z* range for mass spectrometry fragmentation spectra between MC-HilR reference standard (top, orange) and MC-HilR detected in Ingbirchworth reservoir in the September sample (bottom, blue) as head to tail plots. The *m/z* value and the retention time (RT in min) are noted in the title line, HCD 15, 30, 45% stepped normalised collision energy.

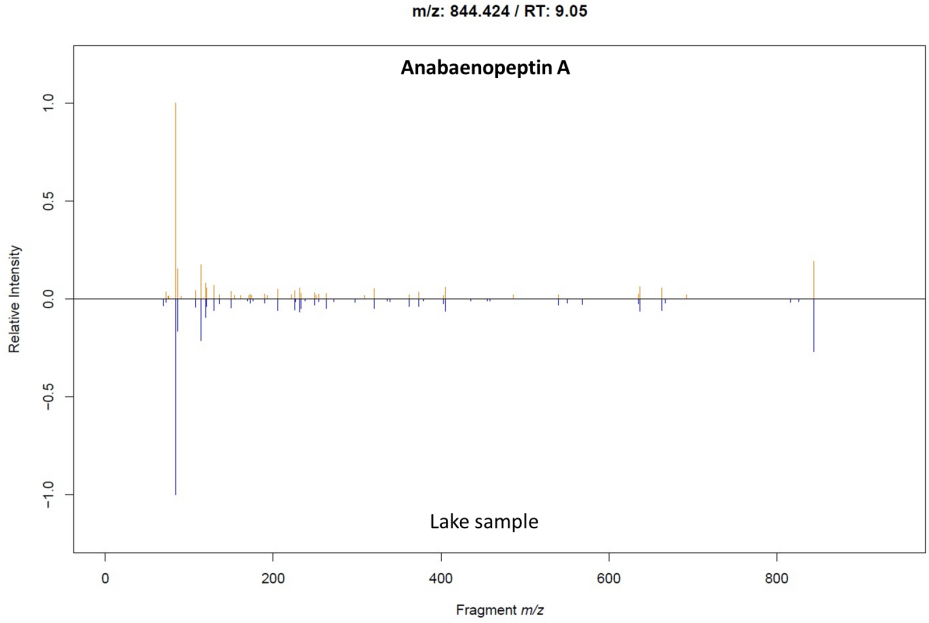

Figure S5. Comparison of relative intensity over *m/z* range for mass spectrometry fragmentation spectra between anabaenopeptin A bioreagent (top, orange) and anabaenopeptin A detected in Ingbirchworth reservoir in the September sample (bottom, blue) as head to tail plots. The *m/z* value and the retention time (RT in min) are noted in the tile line, HCD 15, 30, 45% stepped normalised collision energy.

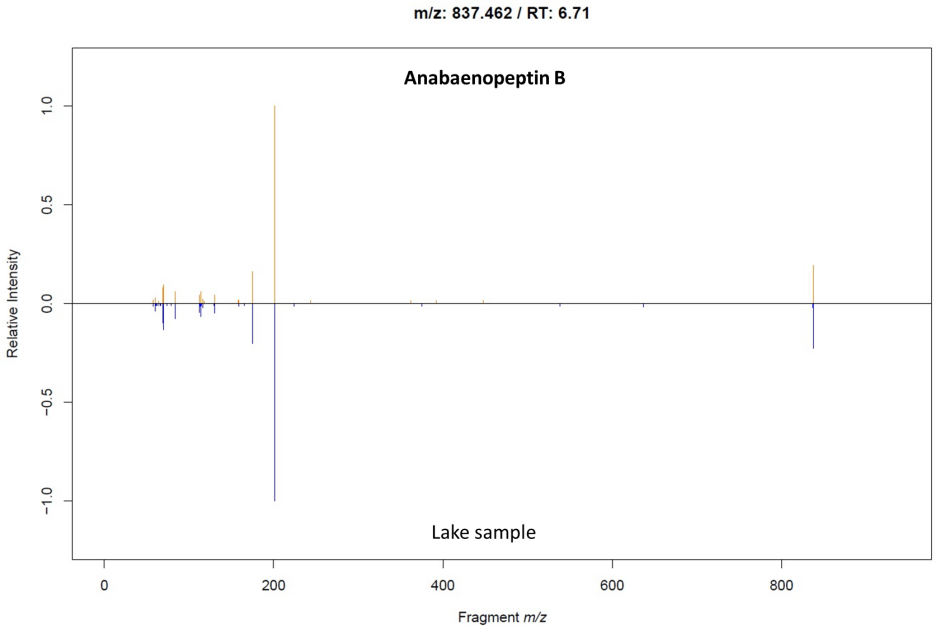

Figure S6. Comparison of relative intensity over *m/z* range for mass spectrometry fragmentation spectra between anabaenopeptin B bioreagent (top, orange) and anabaenopeptin B detected in Ingbirchworth reservoir in the September sample (bottom, blue) as head to tail plots. The *m/z* value and the retention time (RT in min) are noted in the tile line, HCD 15, 30, 45% stepped normalised collision energy.

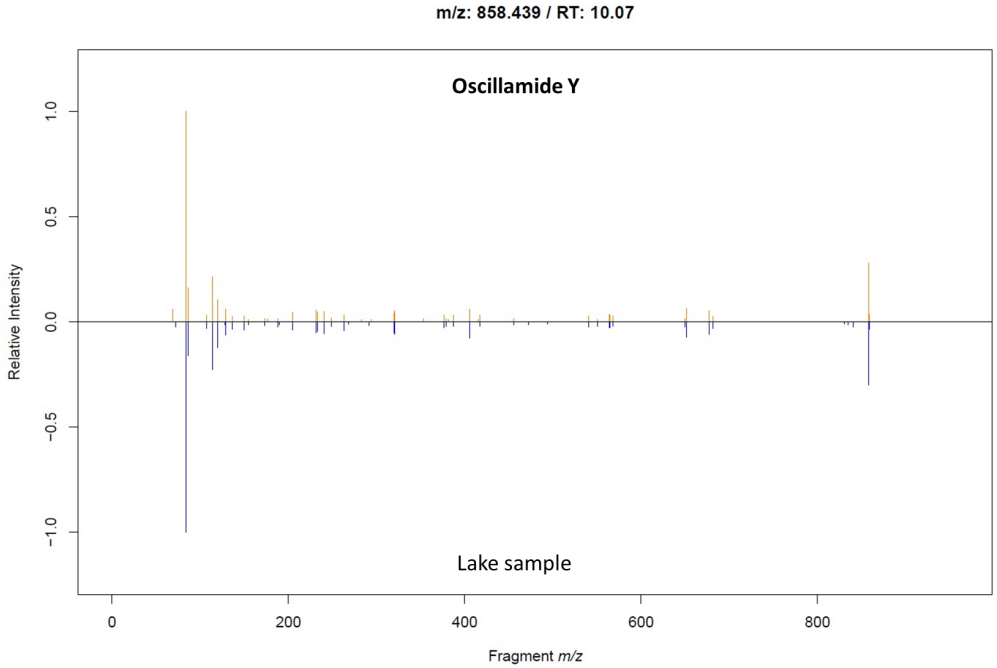

Figure S7. Comparison of relative intensity over *m/z* range for mass spectrometry fragmentation spectra between oscillamide Y bioreagent (top, orange) and oscillamide Y detected in Ingbirchworth reservoir in the September sample (bottom, blue) as head to tail plots. The *m/z* value and the retention time (RT in min) are noted in the tile line, HCD 15, 30, 45% stepped normalised collision energy.

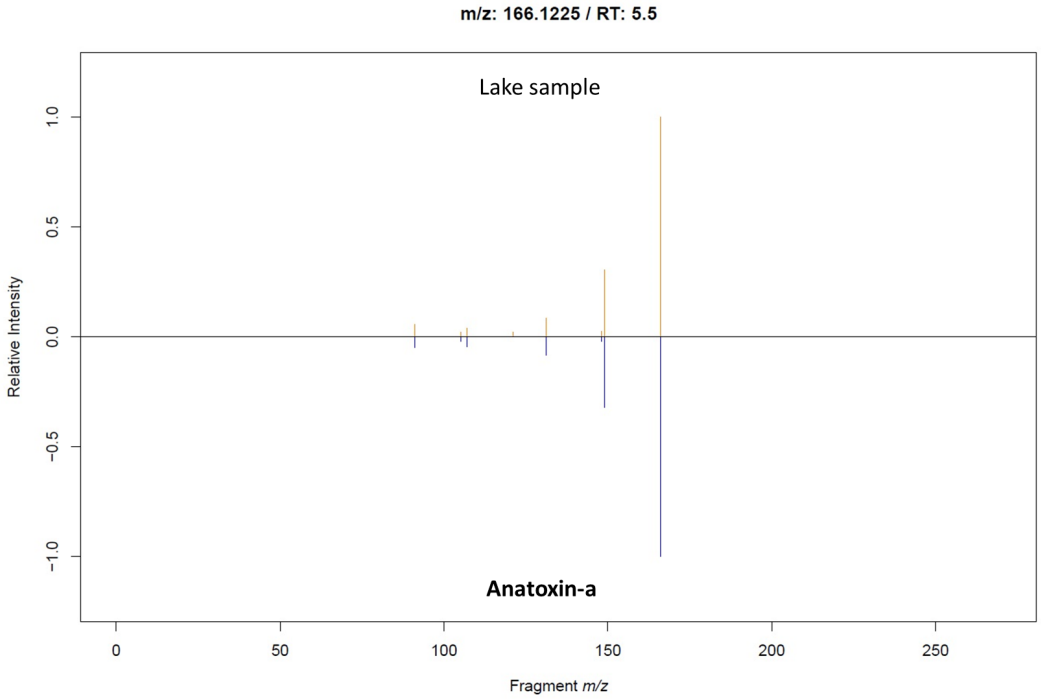

Figure S8. Comparison of relative intensity over *m/z* range for mass spectrometry fragmentation spectra between anatoxin-a reference standard (top, orange) and oscillamide Y detected in Ingbirchworth reservoir in the August sample (bottom, blue) as head to tail plots. The *m/z* value and the retention time (RT in min) are noted in the tile line, HCD – 10 eV.

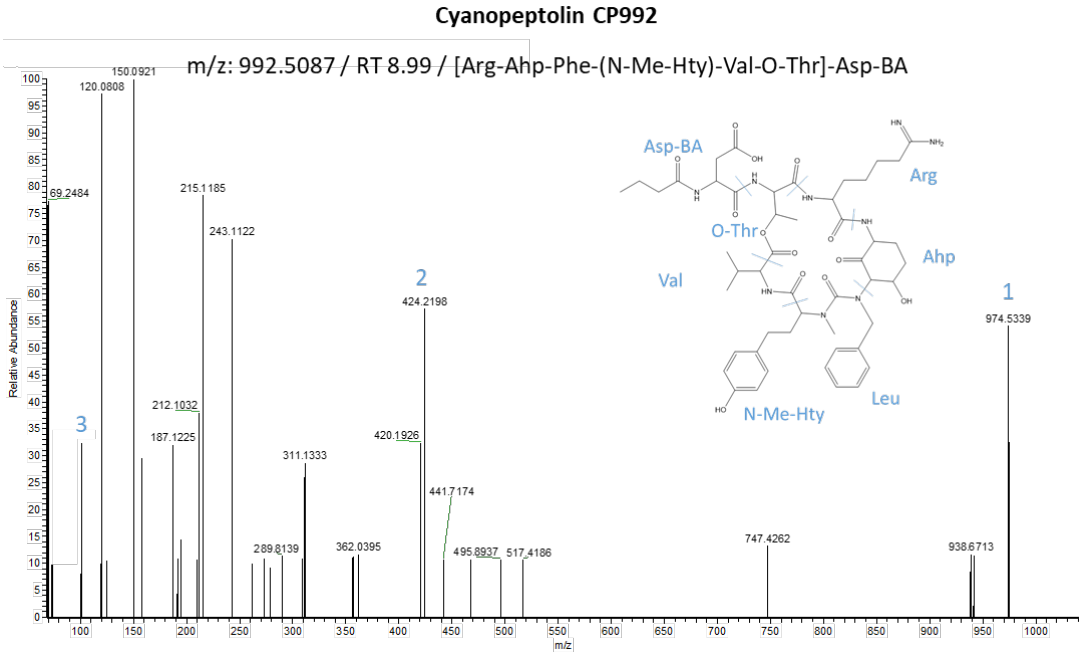

Fragment number	m/z	Fragment
1	974.53	$[M\text{-}H_2O+H]^+$
2	424.22	$[(CO\text{-}Val)\text{-}(N\text{-}Me\text{-}Hty)\text{-}(Leu)]^+$
3	100.04	$[CO\text{-}Val]^+$

Figure S9 Fragmentation spectrum of Cyanopeptolin CP992 detected in Ingbirchworth reservoir in the September sample at HCD 15, 30, 45% stepped normalised collision energy. Precursor *m/z*, retention time (RT) and the building block string are noted at the top. The flat structure is shown with annotated building blocks and sites of fragmentation. The table specifies the *m/z* value and building block fragments that support the identification of this compound.

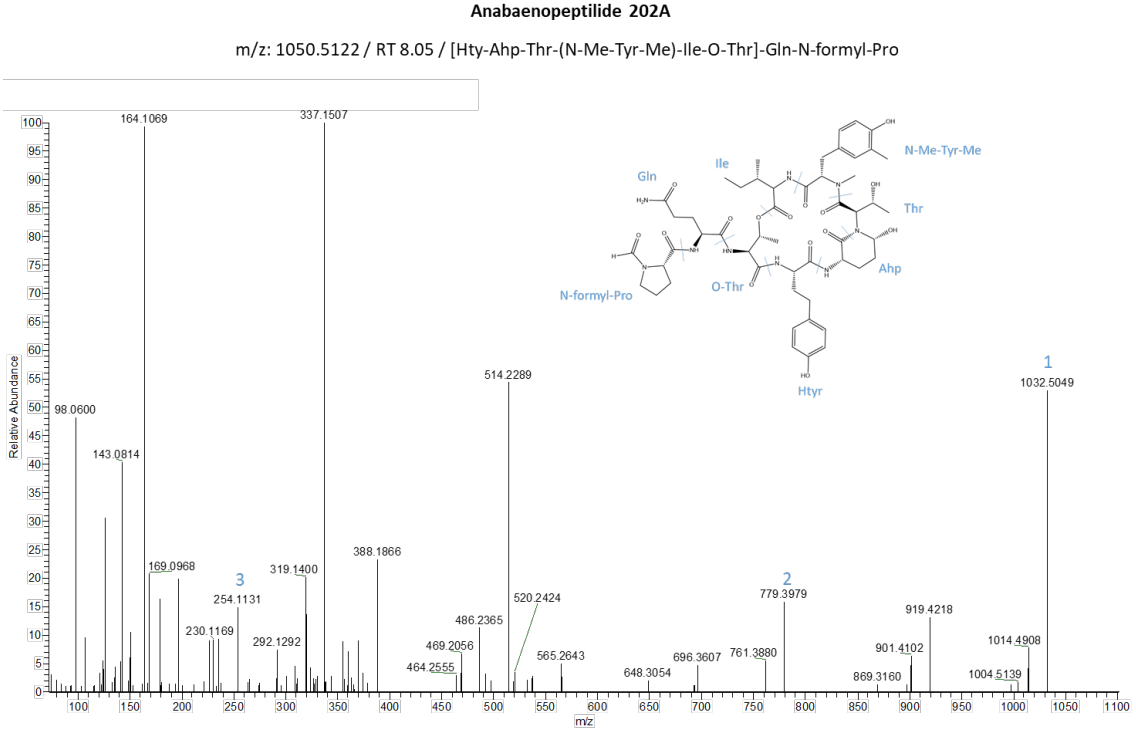

Fragment number	m/z	Fragment
1	1032.50	$[M\text{-}H_2O+H]^+$
2	779.40	$[(O\text{-Thr-Hty-Ahp-Thr-(N-Me-Tyr-Me)-Ile})\text{-}H_2O]^+$
3	254.11	$[CO\text{-Gln-N-formyl-Pro}]^+$

Figure S10. Fragmentation spectrum of Anabaenopeptilide 202A detected in Ingbirchworth **reservoir in the September** sample at HCD 15, 30, 45% stepped normalised collision energy. Precursor *m/z*, retention time (RT) and the building block string are noted at the top. The flat structure is shown with annotated building blocks and sites of fragmentation. The table specifies the *m/z* value and building block fragments that support the identification of this compound.

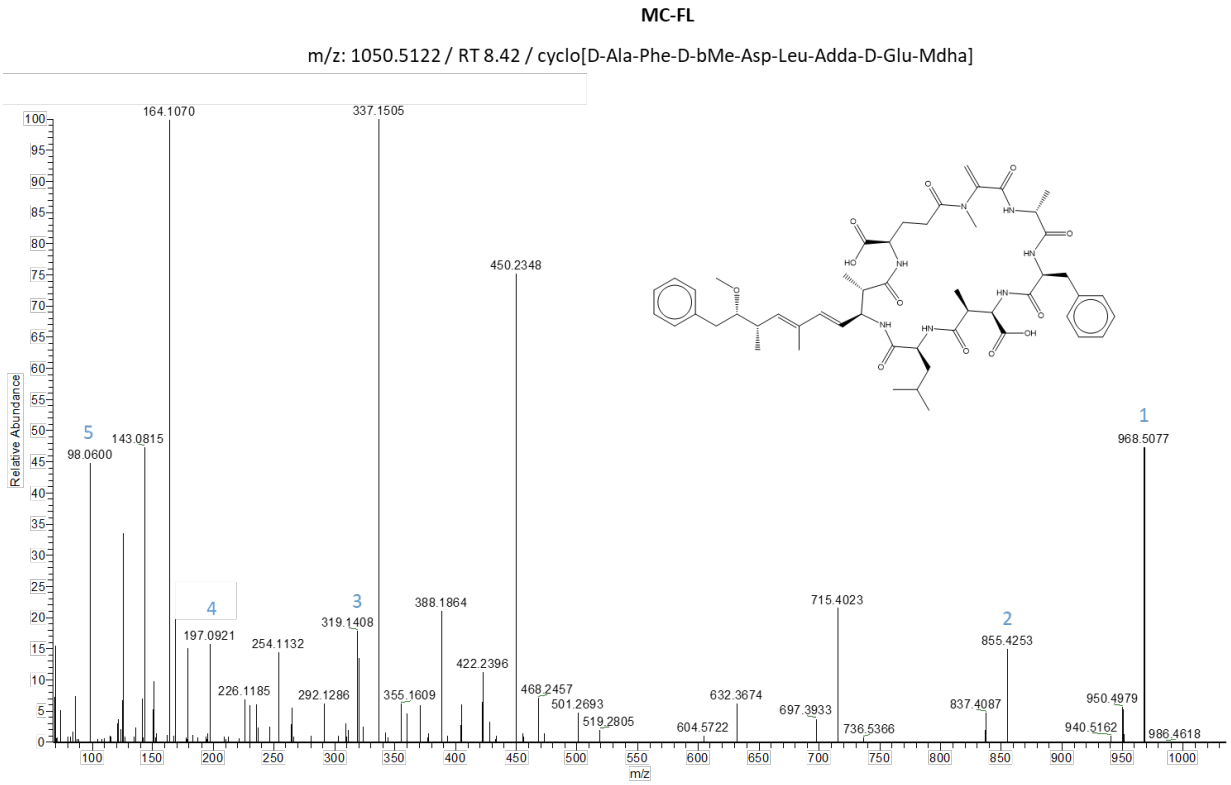

Fragment number	m/z	Fragment
1	968.51	$[M-H_2O+H]^+$
2	855.42	[(Adda-D-Glu-NMe-Dha-D-Ala-Phe-D-bMe-Asp-Leu)-H_2O]$^+$
3	319.17	[NMe-Dha-D-Ala-Phe-D-bMe-Asp]$^+$
4	197.12	[D-bMe-Asp-Leu-Adda]$^+$
5	98.02	[NMe-Dha-D-Ala]$^+$

Figure S11. Fragmentation spectrum of MC-FL detected in Ingbirchworth **reservoir in the September** sample at HCD 15, 30, 45% stepped normalised collision energy. Precursor *m/z*, retention time (RT) and the building block string are noted at the top. The flat structure is shown with annotated building blocks and sites of fragmentation. The table specifies the *m/z* value and building block fragments that support the identification of this compound.